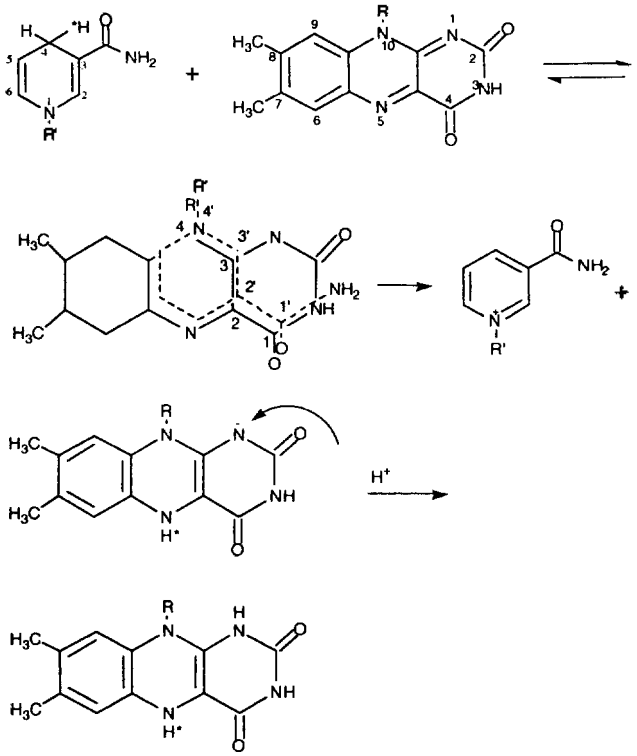

Figure 4. The mechanism of hydride transfer form NADH to flavin.

The charge transfers between other atoms are found to be negligible compared to those between the 1, 2, 3 and 4 positions.

Accordingly, it is proposed that a loose NADH-flavin molecular complex is formed before hydride transfer in the first step, and followed by hydride transfer:

This model nicely explains the fact that hydride at C(4) of NADH transfers to N(5) of flavin.

References

1. (a) Haper, J. David Rawn; Publishers, Row *Biochemistry* **1983**, 412; (b) Christoper Walsh, Freeman, W. H.; Company, *Enzymatic Reaction Mechanism* **1979**, 362.
2. (a) Umeyama, H.; Imamura, A.; Nagata, C. *J. Theoret. Biol.* **1974**, *46*, 1; (b) Eys, J. V.; Stolzenbach, F. E.; Sherwood, L.; Kosower, N. O. *Biochem. Biophys. Acta*, **1958**, *27*, 63; (c) Kosower, E. M. *Biochem. Biophys. Acta*, **1962**, *56*, 474.
3. (a) Nishimoto, K. *Bull. Chem. Soc. Japan* **1967**, *40*, 2493; (b) Song, P. S. *Ann. New York Acad. Sci.* **1969**, *158*, 410.
4. Park, B.-K. *J. Kor. Chem. Soc.* **1980**, *24*, 3.
5. Hoffman, R. *J. Chem. Phys.* **1963**, *39*, 1390.
6. (a) Streitweisser, A. *Molecular Orbital Theory for Organic Chemists*; John Wiley and Sons Inc.: New York, 1961; (b) Fukui *et al., J. Chem. Phys.* **1952**, *20*, 722.
7. (a) Park, B.-K.; Lee, M.-H.; Doh, S.-T. *Bull. Kor. Chem. Soc.* **1985**, *6*, 103; (b) Park, B.-K.; Suh, M.-C. *ibid.* **1986**, *7*, 183.
8. Park, B.-K. 33th seminar in Korean Physical Organic Chemistry 1992.
9. Sutton, L. E.; Phil, M. A. D. *Table of Interatomic Distances and Configuration in Molecules and Ions*; Chemical Society Burlington House: London, 1965.

The Kinetics of Formation and Dissociation of the 1,4,7,10,13,16-Hexaazacyclooctadecane-1,4,7,10,13,16-hexaacetate Complex of Cerium(III)

Ki-Young Choi* and Choon Pyo Hong†

**Department of Chemistry, Mokwon University, Taejeon 301-729*

†*Department of Chemical Education, Kongju National University, Kongju 314-701*

Received November 22, 1993

The formation and dissociation rates of the 1,4,7,10,13,16-hexaazacyclooctadecane-1,4,7,10,13,16-hexaacetic acid (H_6heha) complex of Ce(III) ion have been measured by stopped-flow and conventional spectrophotometry. Observations were made at 25.0± 0.1℃ and at an ionic strength of 0.1 M $NaClO_4$. The formation reaction takes place by rapid formation of an intermediate complex in which the metal ion is incompletely coordinated. In the pH range 4.1-5.2, the H_3heha^{3-} species is the kinetically active one despite of its low concentration. The exchange reaction occurring between the $[Ce(heha)]^{3-}$ complex and Cu^{2+} ion proceeds *via* both an acid-independent and an acid-catalyzed pathway. The buffer concentration dependence of the dissociation rate has also been investigated. The dissociation rate of the $[Ce(heha)]^{3-}$ complex is much faster than that of [Ce(nota)] and $[Ce(dota)]^-$. The chelate ring size effect is discussed by comparing the rate constants to those of analogous nota and dota systems.

Introduction

The lanthanide complexes with the macrocyclic dtpa bis (amide)s and polyazapolycarboxylates, 1,4,7-tris(carboxymethyl)-9,14-dioxo-1,4,7,10,13-pentaazacyclopentadecane (H_3dtpa-eam), 1,4,7-triazacyclononane-1,4,7-triacetic acid (H_3nota), 1,4,

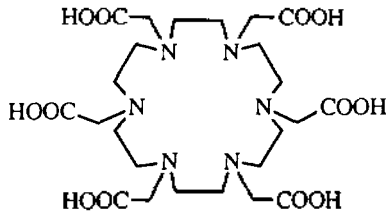

1

Chart 1.

7,10-tetraazacyclododecane-1,4,7,10-tetraacetic acid (H_4dota), and 1,4,8,11-tetraazacyclotetradecane-1,4,8,11-tetraacetic acid (H_4teta) have attracted considerable attention as magnetic resonance imaging (MRI) contrast agents,[1,2] lanthanide ion selective reagents,[3,4] and radiopharmaceuticals.[5] The rates of formation and dissociation of lanthanide complexes with these macrocyclic ligands are found to be much slower than those of analogous linear polyaminepolycarboxylates such as ethylenediaminetetraacetic acid (H_4edta), diethylenetriaminepentaacetic acid (H_5dtpa), and triethylenetetraminehexaacetic acid (H_6ttha).[6,7] This may be attributed to the remarkable rigidity of cyclic aza ring compared with the flexibility of linear complexes. Brucher and Sherry[7] reported that the rate of complexation of $[Ce(dota)]^-$ is slower than that of [Ce(nota)]. This likely reflects the thermodynamic stability by the increased ring size from 9(nota) to 12(dota).[8] Although the difference in thermodynamic stability between $[Ce(teta)]^-$ and [Ce(nota)] is not very significant, [Ce(nota)] dissociates more slowly than $[Ce(teta)]^-$. This is likely a consequence of the destabilizing effect of the 6-membered N-Ce-N chelating by the trimethylenediamine group of the teta ligand.[9] In a thermodynamic study of the complexation of lanthanide with 1,4,7,10,13,16-hexaazacyclooctadecane-1,4,7,10,13,16-hexaacetic acid (H_6heha, **1**) (Chart 1), the stability was found to be less than that of the analogous $[Ln(dota)]^-$ complex.[10] This fact can be explained by the fexibility of the hexaaza ring in **1** compared with the rigidity of the tetraaza ring in dota.

To further understand the factors involved in the chelating kinetics, we have studied the kinetics on the formation and dissociation of Ce(III) complex with **1**.

Experimental

Reagents and solutions. The stock solution of Ce^{3+} was prepared from $CeCl_3$ (Aldrich, 99.9%) and standardized by EDTA titration using Xylenol Orange as an indicator. The ligand **1** was synthesized by the method of Kimura *et al.*[10,11] The concentration of **1** stock solution was determined by titration against a standardized $Cu(ClO_4)_2$ solution using murexide as an indicator. All other chemicals used were of analytical grade and were used without further purification. All solutions were made in deionized water.

Measurements. The ionic strength of the sample solutions was adjusted to 0.1 M with $NaClO_4$. The pH measurements were made by a Beckman Model ϕ 71 pH meter fitted with a combination eletrode. The hydrogen ion concentrations were established from the measured pH value by procedures previously reported.[12] Kinetic measurements were carried out on a Hi-Tech stopped-flow spectrophotometer interfaced with Scientific data acquisition system and a UVI-DEC-610 spectrophotometer at 25.0± 0.1℃ with the use of a Lauda RM 6 circulatory water bath. The working solutions of formation reaction were buffered with 1.0×10^{-2} M sodium acetate/acetic acid. The formation rates of $[Ce(heha)]^{3-}$ were measured by following the change in absorbance of $[Ce(heha)]^{3-}$ at 270 nm, where the absorbance of uncomplexed Ce^{3+} is not significant. The concentration of **1** was 1.0×10^{-4}, while the concentration of Ce^{3+} was varied between 2.0×10^{-4} and 2.0×10^{-3} M. The concentrations of sodium acetate buffer solution of dissociation reaction were varied between 5.0×10^{-3} and 7.5×10^{-2} M. The dissociation rates of $[Ce(heha)]^{3}$ were studied by monitoring the growth in absorbance due to the formation of $[Cu(heha)]^{4-}$ at 270 nm, where Cu^{2+} was used as the scavenger of free ligand. The concentration of $[Ce(heha)]^{3-}$ was 1.0×10^{-4} M while that of the exchanging Cu^{2+} ion was either constant at 1.0×10^{-3} M or it was varied between 2.5×10^{-4} M and 2.5×10^{-3} M.

Table 1. Kinetic Data for Ce(III) Complex Formation Reaction with **1** at 25.0± 0.1℃ and I = 0.1 M ($NaClO_4$)

$10^4[Ce^{3+}]$, M	$10^3\ k_{obs}$, s^{-1}						
	pH 4.12	pH 4.37	pH 4.60	pH 4.75	pH 4.92	pH 5.04	pH 5.14
2.0	0.46	2.00	4.90	8.50	13.33	18.87	25.40
3.0	0.55	2.27	5.40	9.26	14.50	20.40	27.17
4.0	0.62	2.44	5.70	9.70	15.38	21.30	28.20
6.0	0.71	2.70	6.01	10.20	16.13	22.20	29.01
10.0	0.81	2.90	6.31	10.64	16.80	23.26	30.00
20.0	0.87	3.03	6.49	10.87	17.24	23.80	30.77

Results and Discussion

Formation Kinetics. The complex formation of the excess Ce^{3+} ion with **1** can be expressed as

$$Ce^{3-} + HnL^{(6-n)} \rightarrow CeL^{3-} + nH^+ \quad (1)$$

In the pH range 4.1-5.2, H_4L^{2-} is the predominant ligand species in solution. The pH change was kept small by moderate buffering of the solution. The pseudo-first-order rate constants, k_{obs} obtained are shown in Table 1. At a given pH, k_{obs} increased with increasing $[Ce^{3+}]$, exhibiting a saturation curve. The dependence of k_{obs} values on the Ce^{3+} ion concentration can be described by[13]

$$k_{obs} = \frac{k_1 K^* [Ce^{3+}]}{1 + K^* [Ce^{3+}]} \quad (2)$$

where K^* is the stability constant of the intermediate and k_1 is the rate constant for the rate-determining step of the reaction. A similar behavior is also observed for the [Ce(dota)]$^-$ system[6]. On the basis of these results, the formation reaction of $[Ce(heha)]^{3-}$ can be interpreted in terms of Eqs. (3), (4), and (5).

$$Ce^{3+} + H_4L^{2-} \overset{K^*}{\rightleftarrows} (CeH_4L^-)^* \quad (3)$$

Table 2. Rate data for Ce(III) Complex Formation Reaction with **1** at 25.0± 0.1℃ and I=0.1 M ($NaClO_4$)

pH	$10^{-4}K^*$, M^{-1}	k_1, s^{-1}	$10^{-4}k_2$, $M^{-1}s^{-1}$	$\log K_{CeH4L}+^*$
4.12	0.44	0.98	0.43	4.47
4.37	0.80	3.24	2.59	4.49
4.60	1.32	6.77	8.94	4.53
4.75	1.53	11.3	17.3	4.50
4.92	1.45	17.9	26.0	4.39
5.04	1.65	24.6	40.6	4.40
5.14	2.11	31.4	66.3	4.48
				av 4.47± 0.05

$$(CeH_4L^+)^* \xrightarrow{k_1} CeL^{3-} + 4H^+ \quad (4)$$

$$Ce^{3+} + H_4L^{2-} \xrightarrow{k_2} CeL^{3-} + 4H^+ \quad (5)$$

The overall reaction may proceed by a combination of Eqs. (3) and (4), in which a rapidly formed intermediate ($K^*=K_{CeH4L}+^*/K_H$, where $K_H=1+K_5[H^+]+K_5K_6[H^+]^2$) is more slowly rearranged into the final product (k_1). Alternatively, the intermediate is rapidly formed in Eq. (3) but is not on the reaction pathway to the final prduct, which results only from Eq. (5). The values of K^*, k_1, and the second-order rate constant $k_2=K^*k_1$ were calculated from Eq. (2) and summarized in Table 2. The values of $K_{CeH4L}+^*$ can be also evaluated from K^* values obtained at each pH, using known protonation constants of **1**.[10] We formulate the intermediate and its dissociation as in Eqs. (3) and (4) because of the variance of K^* with pH and the dependence of k_1 on $[H^+]^{-1}$ as shown in Table 2. This fact means that the dissociation of the intermediate $(CeH_4L^+)^*$ in Eq. (4) must involve several steps. The second-order rate constant, k_{HnL} (n=3−4) is obtained from the following expression.[14]

$$k_2=k_{HnL}\,(1+K_{H(n+1)L}\,[H^+])^{-1} \quad (6)$$

where $K_{H(n+1)L}$ is the protonation constant of **1**. From the plots of k_2 *vs.* $(1+K_{H(n+1)L}\,[H^+])^{-1}$, the second-order rate constants, k_{H3L} and k_{H4L} for the H_3L^{3-} and H_4L^{2-} species obtained are (8.0± 0.7)×10^8 and (7.8± 1.4)×10^5 $M^{-1}s^{-1}$, respectively. Despite of its very low concentration in the pH range studied, the H_3L^{3-} species appears to be kinetically more reactive than the tetraprotonated species H_4L^{2-}, even though the latter is the predominant species in solution. The same conclusion was reported previously by Wilkins *et al.*[14] The stability constant, $K_{CeH4L}+^*$ of the intermediate complex obtained here is larger than that for the corresponding triacetate complexes.[15] This indicated that Ce^{3+} ion may be coordinated to more than three carboxylated groups in the intermediate. Thus, we propose that at least four carboxylate groups and perhaps two nitrogen in **1** are coordinated to the Ce^{3+} ion in the protonated intermediate complex $(CeH_4L^+)^*$.

Dissociation Kinetics. Since the stability constant of $[Ce(heha)]^{3-}$[10] is 4 orders of magnitude lower than that of $[Cu(heha)]^{4-}$, the displacemant of Ce^{3+} ion from the $[Ce(heha)]^{3-}$ complex is complete in the presence of excess Cu^{2+} ion. The rates of this exchange reaction have been measured between pH 4.0 and 5.0. In the presence of excess

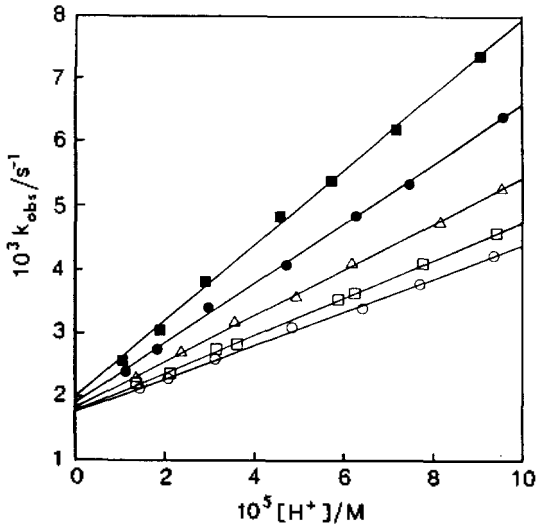

Figure 1. Plots of k_{obs} *vs.* $[H^+]$ for the dissociation kinetics of $[Ce(heha)]^{3-}$ with Cu(II) at different buffer concetrations. ($[Ce(heha)]^{3-}=1.0\times10^{-4}$ M, $[Cu^{2+}]=1.0\times10^{-3}$ M, T=25.0± 0.1 ℃, I=0.1 M ($NaClO_4$); $[Ac^-]$: 5.0 mM (○); 10.0 mM (□); 25.0 mM (△); 50.0 mM (●); 75.0 mM (■).

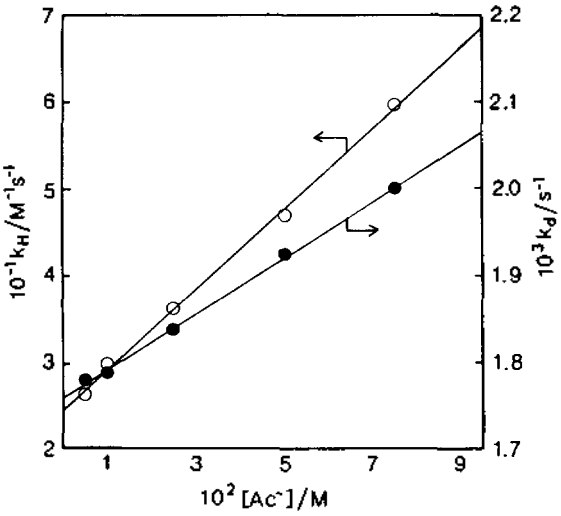

Figure 2. Plots of k_H (○) and k_d (●) *vs.* $[Ac^-]$ for the dissociation kinetics of $[Ce(heha)]^{3-}$ with Cu(II). ($[Ce(heha)]^{3-}=1.0\times10^{-4}$ M, $[Cu^{2+}]=1.0\times10^{-3}$ M, T=25.0± 0.1℃, I=0.1 M ($NaClO_4$).

Cu^{2+} ion, the rate of exchange may be expressed as

$$-d\,[CeL^{3-}]/dt=k_{obs}\,[CeL^{3-}] \quad (7)$$

where k_{obs} is a pseudo-first-order rate constant. The observed rate constant, k_{obs} was found to be independent of $[Cu^{2+}]$. The dependences of the observed rate constants upon $[H^+]$ at various acetate buffer concentrations are shown in Figure 1. For each case, a linear least-square fit of these plots had a non-zero intercept which is consistent with the exchange reaction proceeding *via* both an acid-independent and an acid-dependent pathways. Thus, the kinetic data can be described by

$$k_{obs}=k_d+k_H[H^+] \quad (8)$$

Table 3. Rate Constants for the Exchange Reaction of CeL/Cu^{2+} at 25.0± 0.1℃ and I=0.1 M ($NaClO_4$).

Exchange reaction	Rate term	Rate constant	Ref.
$[Ce(heha)]^{3-}$ /Cu^{2+}	$k_1[CeL^{3-}]$	$(1.76\pm 0.03)\times 10^{-3}$ s^{-1}	
	$k_2[CeL^{3-}][Ac^-]$	$(3.26\pm 0.07)\times 10^{-3}$ M^{-1} s^{-1}	
	$k_3[CeL^{3-}][H^+]$	$(2.44\pm 0.05)\times 10^{1}$ M^{-1} s^{-1}	
	$k_4[CeL^{3-}][H^+][Ac^-]$	$(4.61\pm 0.12)\times 10^{2}$ M^{-2} s^{-1}	
[Ce(nota)] /Cu^{2+}	$k_1[CeL]$	$(2.5\pm 0.3)\times 10^{-5}$ s^{-1}	
	$k_2[CeL][H^+]$	$(4.3\pm 0.5)\times 10^{-2}$ M^{-1} s^{-1}	7
$[Ce(dota)]^-$ /Cu^{2-}	$k_1[CeL^-][H^+]$	$(8\pm 2)\times 10^{-4}$ M^{-1} s^{-1}	6
	$k_4[CeL^-][H^+]^2$	$(2\pm 1)\times 10^{-3}$ M^{-2} s^{-1}	

Figure 2 shows that k_d and k_H are directly proportional to the total acetate buffer concentration after correction for the formation of copper acetate complexes.[16] The enhanced rates in the presence of higher acetate buffer concentration may be attributed to the acetate ion complexation. If a ternary complex, $[Ce(heha)ac]^{4-}$ is present, it is probably more sensitive than binary $[Ce(heha)]^{3-}$ to be attacked by the hydrogen ions. Based on the data, the overall rate of reaction may be expressed as

$$-d[CeL^{3-}]/dt = k_1[CeL^{3-}] + k_2[CeL^{3-}][Ac^-] + k_3[CeL^{3-}][H^+] + k_4[CeL^{3-}][H^+][Ac^-] \quad (9)$$

Values of the specific rate constants, k_n ($n=1-4$), calculated from a weighted least-square program, are listed in Table 3. Table 3 also includes the rate constants for the dissociation of related Ce(III)-polyazapolycarboxylates. The data indicate that the dissociation of $[Ce(heha)]^{3-}$ follows a similar mechanism to the dissociation of lanthanide complexes with other polyaza[7,17] and polyaminepolycarboxylates.[18,19] In these reactions, the Ce-carboxylate bonds are rapidly forming and breaking, allowing attachment of H^+ or Cu^{2+} to a dissociated carboxylate. Presumably, the slow step involved the rupture of a Ce-N bond subsequent to formation of $CeLH^{2-}$ or $CeLCu^-$ intermediate.

The effect of the ligand on the dissociation rate constant can be seen by comparing the values in Table 3 along with the other Ce(III)-polyaza polycarboxylates. The acid-catalyzed rate constant of [Ce(nota)] was found to be about fifty times larger than that of the $[Ce(dota)]^-$ complex. An increase in ring size from 9 (nota) to 12 (dota) leads to an increase in kinetic stability because of remarkable rigidity of the tetraaza (dota) compared with the triaza (nota) macrocycles. However, $[Ce(heha)]^{3-}$ dissociates about 2 or 4 orders of magnitude faster than that of [Ce(nota)] and $[Ce(dota)]^-$, even though 1 has the greatest number of donor atoms (N and O) and the increased ring size (18-membered cycle) compared with nota and dota. This indicates that the acid-catalyzed rate of $[Ce(heha)]^{3-}$ may be attributed to the decrease of macrocycle rigidity by the flexibility of hexaaza ring (1) compared with tetraaza ring (dota) and the lesser degree of net chelation. Thus, we have included log $\beta_{Ce(heha)^{3-}}$ in linear correlation of stability of several Ce(III)-aminopolycarboxylate complexes[15] (5-membered O-Ce-N) *vs.* ΣpK_a in Figure 3. This correlation represents that the complexing properties of a ligand are in keeping with the behavior of analogous chelates. The value of **1** falls far off the correlation line, indicating that the Ce^{3+} ion is not coordinated to all the possible donors in **1**. This could reflect the absence of bonding between the Ce^{3+} ion and some carboxylate groups. However, the highest pK_a for carboxylate group in **1** is 4.64 and the deviation from the correlation corresponds to about 19 units of ΣpK_a. This indicates that some N donors may not bound. Based on the dissociation kinetic data as well as on the deviation of the stability constant from the log β *vs.* ΣpK_a correlation, we propose that the Ce^{3+} ion is bound to some carboxylate groups and two nitrogen atoms in **1**.

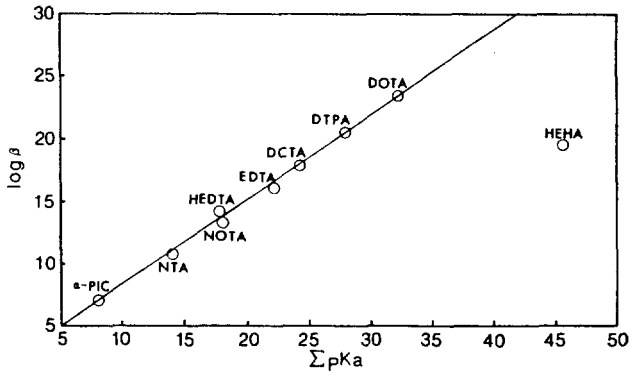

Figure 3. Plots of log β *vs.* Σ pK_a for Ce(III)-aminopolycarboxylate complexes at 25.0± 0.1℃, and 0.1 M ionic strength.

Acknowledgment. This paper was supported by NON DIRECTED RESEARCH FUND, Korea Research Foundation, 1993.

References

1. Sherry, A. D.; Singh, M.; Geraldes, C. F. G. C. *J. Magn. Reson.* **1986**, *66*, 511.
2. Lauffer, R. B. *Chem. Rev.* **1987**, *87*, 901.
3. Hagan, J. J.; Taylor, S. C.; Tweedle, M. F. *Anal. Chem.* **1988**, *60*, 514.
4. Carvalho, J. F.; Kim, S. H.; Chang, C. A. *Inorg. Chem.* **1992**, *31*, 4065.
5. Wedeking, P.; Tweedle, M. F. *Nucl. Med. Biol.* **1988**, *15*, 395.
6. Brucher, E.; Laurenczy, G.; Makra, Z. S. *Inorg. Chim. Acta.* **1987**, *139*. 141.
7. Brucher, E.; Sherry, A. D. *Inorg. Chem.* **1990**, *29*, 1555.
8. Cacheris, W. P.; Nickel, S. K.; Sherry, A. D. *Inorg. Chem.* **1987**, *26*, 958.
9. Choi, K. Y.; Kim, J. C.; Kim, D. W. *J. Coord. Chem.* **1993**, *30*, 1.
10. Kodama, M.; Koike, T.; Mahatma, A. B.; Kimura, E. *Inorg. Chem.* **1991**, *30*, 1270.
11. Kimura, E.; Fujioka, H.; Yatsunami, A.; Nihira, H.; Kodama, M. *Chem. Pharm. Bull.* **1985**, *33*, 655.

12. Muscatello, A. C.; Choppin, G. R.; D'Olieslager, W. *Inorg. Chem.* **1989**, *28*, 993.
13. Wilkins, R. G. *The Study of Kinetics and Mechanisms of Reactions of Transition Metal Complexes*; Allyn and Bacon, Inc.: Boston, 1974; Chap. 1.
14. Kasprzyk, S. P.; Wilkins, R. G. *Inorg. Chem.* **1982**, *21*, 3349.
15. Martell, A. E.; Smith, R. M. *Critical Stability Constants*; Plenum Press: New York, 1989; Vol. 6.
16. DeJongh, M.; D'Olieslager, W. *Inorg. Chim. Acta.* **1985**, *109*, 7.
17. Choi, K. Y.; Kim, K. S.; Kim, J. C. *Bull. Chem. Soc. Jpn.* **1994**, *67*, 267.
18. Choi, K. Y.; Choppin, G. R. *Inorg. Chem.* submitted for publication.
19. Choi, K. Y.; Choppin, G. R. *J. Coord. Chem.* **1991**, *24*, 19.

Crystal Structures of Zeolitic Water Molecules in Cs_3Na_9-A and Cs_3Na_8H-A

Kee Heon Cho, Jin Hyun Kwon, Hae Won Kim†
Chong Sam Park,‡ and Nam Ho Heo*

Department of Industrial Chemistry, Kyungpook National University, Taegu 702-701
†Department of Industrial Chemistry, Kyungpook Sanup University, Taegu 701-702
‡Department of Radiotechnology, Taegu Junior Health College, Taegu 702-260
Received December 2, 1993

Structures of zeolitic water molecules in hydrated Cs_3Na_9-A and Cs_3Na_8H-A have been studied by single-crystal x-ray diffraction methods in the cubic space group $Pm\bar{3}m$ at 21℃. In the crystal structure of fully dehydrated Cs_3Na_9-A (a=12.265(1) Å with R_1=0.056 and R_2=0.057), nearly three and eight Cs^+ and Na^+ ions per unit cell are found at the centers of 8- and 6-oxygen rings with closest approaches of 3.401(11) and 2.303(6) Å to framework oxygens, respectively. The twelfth Na^+ is located opposite 4-oxygen ring in the large cavity with an occupancy of 0.6(2). The crystal structures of hydrated Cs_3Na_9-A (a=12.273(1) Å with R_1=0.065 and R_2=0.078) and Cs_3Na_8H-A (a=12.286(1) Å with R_1=0.078 and R_2=0.081) are viewed as having two kinds of unit cells, $Cs_3Na_{9-x}H_x$-A·$20H_2O$ and $Cs_3Na_{9-x}H_x$-A·$24H_2O$ (x=0 and 1, respectively), each with different secondary structures of zeolitic water molecules in its large cavity. In both unit cells, Cs^+ ions are found at centers of 8-rings with large thermal parameters, showing changes in their coordination environments due to approaches of water molecules upon hydration. Na^+ ions on 6-rings have also changed their geometries from trigonal to tetrahedron upon hydration, each with three framework oxygens at 2.356(11) Å and an additional zeolitic water molecule at 2.18(3) Å on a threefold axis which is perpendicular to the 6-ring of the framework oxygens. In the large cavity of $Cs_3Na_{9-x}H_x$-A·$20H_2O$, four water molecules are arranged tetrahedrally on the threefold axes, each in trun with tetrahedrally coordinated three water molecules at 2.83(6) Å. In the case of $Cs_3Na_{9-x}H_x$-A·$24H_2O$, eight waters molecules on the threefold axes occupy eight symmetry equivalent positions, each in trun with tetrahedrally coordinated three waters at 2.51(6) Å, resulting in a pseudo-dodecahedron of twenty water molecules with twelve shared and distorted pentagons perturbed by approaches of Cs^+ ions. Four water molecules in each sodalite unit of both crystals are arranged tetrahedrally and seem to have weaker interactions with the Na^+ ions on 6-rings due to the stronger interactions between the Na^+ ions and the water molecules in the large cavity.

Introduction

Unlike other guest molecules in the molecular-dimensioned cavities of zeolites, water molecules tend to make bonds to both exchangeable cations and framework oxide anions by donating lone-pair electrons to the empty orbitals of cations and hydrogens to the framework oxide anions, respectively. Accordingly, their distances from cations and framework atoms are limited within their normal and hydrogen bonding distances, especially when they are located within the primary coordination spheres of the zeolitic cations and framework atoms. Such zeolitic water molecules are sometimes found to be a part of secondary and tertiary structures, which are usually found in the molecular-dimensioned channels and cavities with appropriate volumes.[1,2] As stable secondary structures suggested by many theoretical chemists,[3,4] pentagons of water molecules were actually found crystallographically in narrow hydrophilic regions of hydrophobic protein[1] as well as in the cavities of zeolite A.[2] Helical arrangement of water molecules was also reported in the channels of hydrated VPI-5 zeolite.[5] However, the presence of tertiary structures of water molecules, such as helical strands and dodecahedron, is so far suggested only in the highly symmetrical channels and cavities of hydrated zeolites.[2,5]